1974

Experimental Evaluation of a Scotch-Yoke Compressor Mechanism

J. P. Elson
Copeland Corporation

J. J. Amin
Copeland Corporation

EXPERIMENTAL EVALUATION OF A SCOTCH-YOKE COMPRESSOR MECHANISM

J. P. Elson, Project Engineer
Copeland Corporation, Sidney, Ohio 45365

J. J. Amin, Instrumentation Engineer
Copeland Corporation, Sidney, Ohio 45365

INTRODUCTION

A Scotch-yoke mechanism is known to generate a pure harmonic motion. Kinematically, it is equivalent to the slider crank mechanism of conventional reciprocating compressors when the connecting rod is imagined to have an infinite length. Since pure harmonic motion is generated, shaking forces occur only at the fundamental running frequency of the compressor and perfect dynamic balance is possible. This feature plus a compact design are the major advantages of a Scotch-yoke mechanism in compressor design.

Until recently, Scotch-yoke mechanisms have been utilized only in compressors of relatively small capacity. For the application discussed herein, a Scotch-yoke mechanism has been employed in a line of four cylinder hermetic compressors ranging in capacity from 90,000 BTUH to 145,000 BTUH. With this design, two pair of opposed pistons are employed perpendicular and in slightly offset planes. Figure 1 illustrates the general layout of one pair of these pistons and the corresponding Scotch-yoke mechanism.

As illustrated in Figure 1, an eccentric shaft (1) drives block (2), which in turn drives the yoke and piston assembly with a pure harmonic motion. To achieve lightweight construction, aluminum was employed for these components and a Swedish steel bearing strip (6) was then used to minimize friction and wear. To hold the bearing strip to the yoke, a steel rivet (7) was used. To complete the assembly, a retainer (5) was employed to guide the block in the yoke.

The design analysis of the above mechanism included consideration of three major components: the shaft, the slider block, and the yoke assembly. Of these, the determination of operating stress levels in the yoke assembly presented the most difficult and unique problem. Thus, in the following, several analysis techniques are described which employ both experimental and analytical means to determine operating stress levels for the yoke. With the first method, experimental cylinder pressure data is used in conjunction with a static load fixture to simulate operating loads on the yoke. Stress levels are then calculated at various yoke locations using experimental strain data. With the second method, dynamic strains are measured on the operating yoke through the use of a special linkage which allows the transport of strain gage wires from the yoke to the compressor body. Yoke strains measured in this manner are then compared with the result obtained from the static strain analysis.

Both of the methods described above were utilized in the development of the yoke. Due to the straightforeward measurements of the static strain method, minor design changes in the yoke were evaluated by this method. The second method was then used to verify the general correctness of the more approximate first method and also, to evaluate the final yoke design. The tedious installation and short life (15 to 30 minutes) of the strain gage wiring used in the operating compressor prohibited the use of the second method as a practical development tool. As will be shown, the static strain measurements agreed well with those obtained from the operating compressor.

STATIC STRAIN MEASUREMENTS

As an initial step towards the analysis of the yoke, a free body diagram of the yoke-piston assembly was constructed as shown in Figure 2. Included here are cylinder pressure loads from both cylinders, F_1 and F_2, an inertia force, F_i, a reaction force between the slider block and yoke, F_b, and the side reaction forces, R, on the pistons. Neglected in this diagram are frictional forces which were estimated to be of minor importance. Summing forces in the direction of motion yields:

$$F_b = F_1 - F_2 - F_i \qquad (1)$$

where

$$F_1 = P_1 A$$

$$F_2 = P_2 A$$

$$F_i = me\omega^2 \cos\theta$$

and

P_1 = pressure in cylinder 1, psia

P_2 = pressure in cylinder 2, psia

A = piston area, in^2

e = compressor crank eccentricity, in.

m = yoke-piston assembly mass, $lb_f sec^2/in.$

ω = compressor radian frequency, rad/sec.

θ = compressor crank angle, rad.

Due to the offset nature of the force, F_b, the yoke must withstand a torsional load, T, which is balanced by the piston reaction, R.

$$T = F_b e \sin \theta \qquad (2)$$

This torque constitutes the major loading on the yoke and, therefore, was used as the basis of an experiment for static strain measurements. When F_b from Equation (1) becomes less than zero, the slider block loading transfers to the piston 2 side of the yoke which then experiences torque, T. Equation (2) is valid for torques on both sides of the yoke with the counterclockwise direction being defined as positive.

To identify maximum stress regions in the specific yoke-piston assembly, a photostress model was constructed and loaded according to the geometry shown in Figure 2. From the analysis of this model surface stress was identified to be maximum at the rivet and fillet cross sections of the yoke. Strain gages were then installed at these locations and a static load fixture was constructed as shown in Figure 3. To apply a torque to the yoke, it was necessary to first replace the pistons by bolts of sufficient length to simulate the location of the piston side forces, R. A special nut was then fit over the yoke and a torque of known magnitude was applied with a standard torque wrench. Since a torque wrench applies both a torque and a force, it was necessary to average two strain readings at each location, one before and one after a 180° rotation of the wrench. The subscripts 1 and 2 used with torque, T, in Figure 3, denote the side of the yoke on which the torque was applied.

Data was taken for positive and negative torques and for several torque levels considered representative of the actual torques experienced by the yoke in the operating compressor. Since the strain at all locations was found to be proportional to the applied torque, the data given below is presented to terms of a strain per unit torque, α_j, (μ in/in/ft-lb).

TABLE 1

EXPERIMENTAL STRAIN DATA - UNIT TORQUE

Torque	α_1	α_2	α_3	α_4
T_1	9.75	5.87	-9.56	-10.4
T_2	1.00	5.31	-9.69	- 2.46

To calculate actual operating strains, cylinder pressure data was measured and used in conjunction with Equation (2) to calculate torque as a function of crank angle. Then, using Table 1, operating compressor strain, ϵ_j (μ in/in), was calculated from the equation:

$$\epsilon_j = \alpha_j T \qquad j = 1, 2, 3, 4 \qquad (3)$$

For $F_b > 0$, α_j was selected according to torque, T_1, while for $F_b < 0$, α_j was selected according to T_2.

In addition to the applied torque described above, the yoke must also withstand a compression loading due to inertia. Specifically, as the yoke decelerates toward top or bottom dead center, the inertia force generated in the unloaded side of the yoke places the yoke in compression. This compression force, termed F_c, has a maximum value of roughly one-half the total inertia force in the yoke-piston assembly and may be defined mathematically by the equation:

$$F_c = \frac{me\omega^2}{2} |\cos \theta| \qquad (4)$$

To model this effect with a static experiment, the yoke-piston assembly was loaded in compression and unit strains, β_j (μ in/in/lb) were determined, as given below, for each strain gage location.

$\beta_1 = -0.80 \quad \beta_2 = 0.15 \quad \beta_3 = 1.00 \quad \beta_4 = -0.60$

The above strain effect was superimposed with that given by Equation (3) to yield a final equation for the total predicted strain.

$$\epsilon_j = \alpha_j T + \beta_j F_c \qquad j = 1, 2, 3, 4 \qquad (5)$$

Both terms in Equation (5) were considered significant, however, the maximum value of the first term was about four times the maximum of the second term.

DYNAMIC STRAIN MEASUREMENT

The strain gage installation used for dynamic measurements is illustrated in Figures 4 and 5. Due to the straight-line motion of the yoke-piston assembly, it was possible to use a single wire-carrying beam to transport the strain gage wiring from the moving yoke-piston assembly to a muffler cover attached to the compressor body. With this mechanism, the yoke to beam wiring must endure a rotation of the carriage beam of ± 15° relative to the yoke. At the muffler cover, the wiring experiences only minor translation and rotation when the wires are located as shown in Figure 4.

Due to the high speed (3500 rpm) of the instrumented compressor, great care was required to minimize unnecessary motion of the wiring. Two factors which helped significantly to accomplish this are as follows. First, the wires at the yoke were brought through a single hole as close to the pin joint as possible. Second, the wires at the muffler cover were brought through a hole in the beam at a point of minimal motion. Even with these modifications, the best life obtained with this

instrumentation system was 30 min. This, however, was more than adequate to obtain the required data.

COMPARISON OF STATIC AND DYNAMIC STRAINS

For the dynamic strain measurements, gage locations 1 and 2 of Figure 3, were selected for comparison with the static strain predictions. Gage locations 3 and 4 were not selected due to their inaccessible location during dynamic operation. Figures 6 and 7 show the degree of correlation obtained between the static strains calculated from Equation 5, and the dynamic strain measurements at locations 1 and 2 respectively. At location 2, the agreement is excellent while at location 1, the agreement is quite good in terms of peak strain. The major disagreement between the static and dynamic strains at location 1 occurs when the block loading force shifts from one side of the yoke to the other. Under this condition, which occurs approximately 30° after top and bottom dead center, a minor impact causes dynamic strain which was not allowed for in the static model. However, in terms of peak measured strain, this impact strain is insignificant. Based on the good agreement shown by Figures 6 and 7, the static model was assumed valid and maximum strains were calculated at the four instrumented locations as shown in Table 2 below.

TABLE 2

MAXIMUM YOKE STRAIN

Location	Crank Angle, θ	$\varepsilon_{max.}$
1	300	- 393
2	300	- 196
3	300	+ 394
4	300	+ 349

Two conclusions may be drawn from Table 2. First, the maximum yoke strain (+394) occurs at location 3, and second, the yoke strain does not vary significantly in going from the fillet to rivet hole cross sections. This latter conclusion was considered most desirable in that minimizing stress gradients was considered an important objective of this investigation. A second objective of this investigation, and certainly the most important one, was to determine whether yoke stress levels were excessive. To do this, the maximum stress level in the yoke was estimated from the equation:

$$\sigma = E\,\varepsilon \qquad (6)$$

where

σ = stress, psi

E = modulus of elasticity, psi

For the aluminum yoke, a value for E of 10.6×10^6 was used to calculate a peak stress at location 3 of 4175 psi. This was considered more than safe in that the aluminum employed has an endurance strength of 18,000 psi compared to the 4175 psi calculated above for a standard operating condition of the compressor.

SUMMARY AND CONCLUSIONS

A calculation method, employing static strain and cylinder pressure measurements, was presented for the prediction of dynamic strains on the yoke member of a Scotch-yoke compressor mechanism. The calculation method was evaluated by comparing the predicted results with actual dynamic strain measurements obtained from an operating compressor. Good agreement was shown and peak stress levels were identified with the aid of the calculation method. The instrumentation technique used in determining dynamic strains, was illustrated in detail.

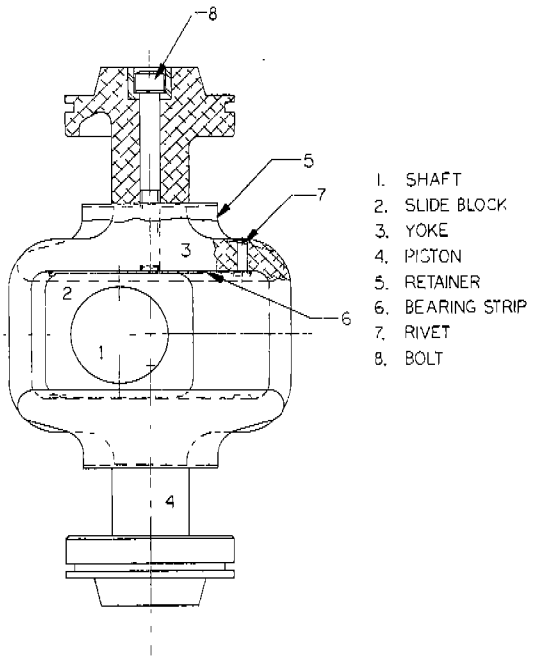

Figure 1. Compressor Scotch-Yoke Mechanism.

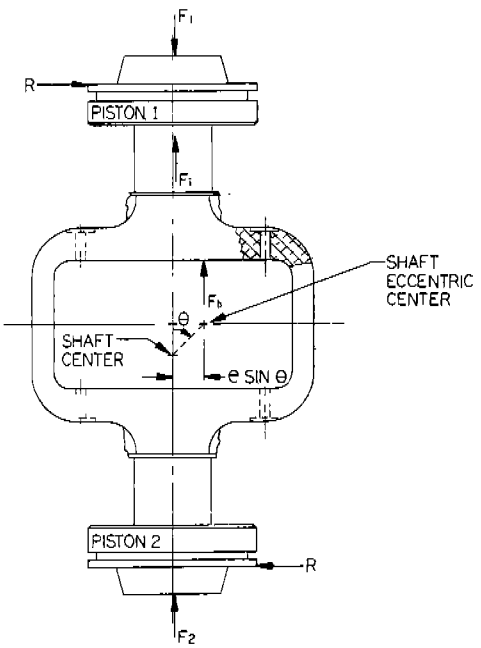

Figure 2. Loading Diagram, Yoke-Piston Assembly.

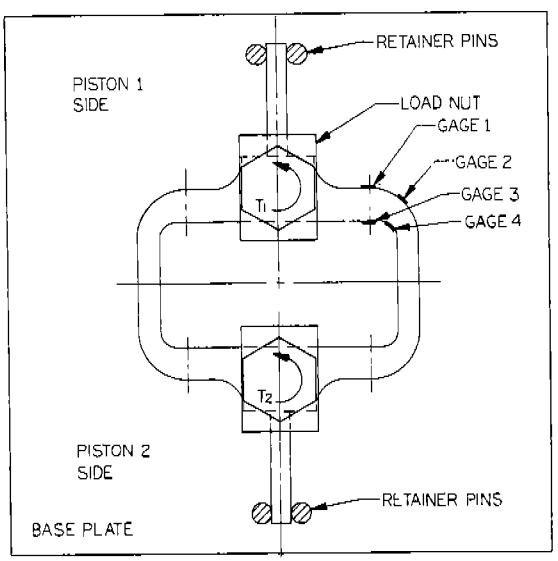

Figure 3. Static Strain Load Fixture.

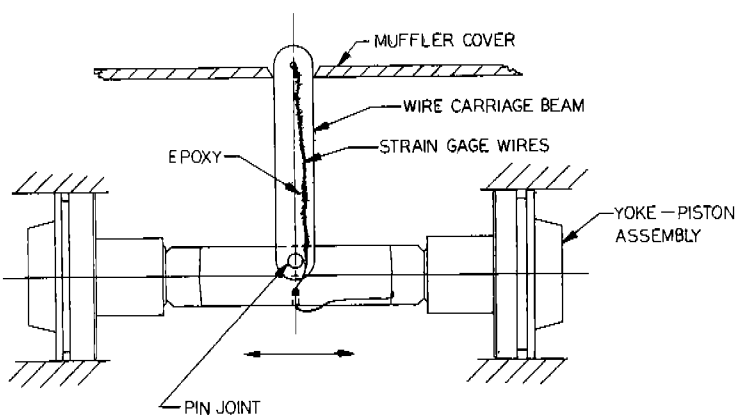

Figure 4. Dynamic Strain Measurement Mechanism.

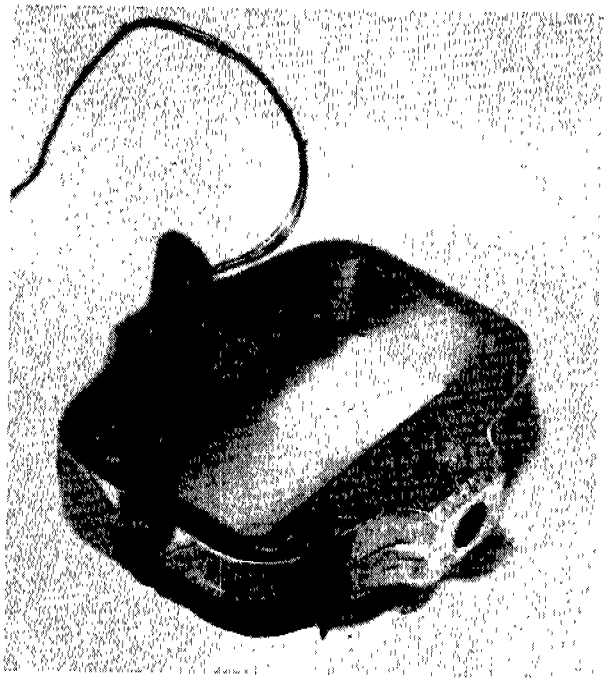

Figure 5. Yoke Strain Gage Wiring.

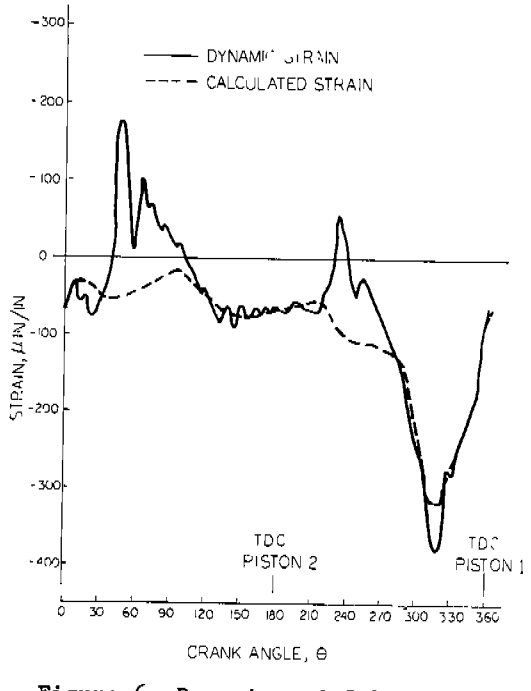

Figure 6. Dynamic and Calculated Strain at Location 1.

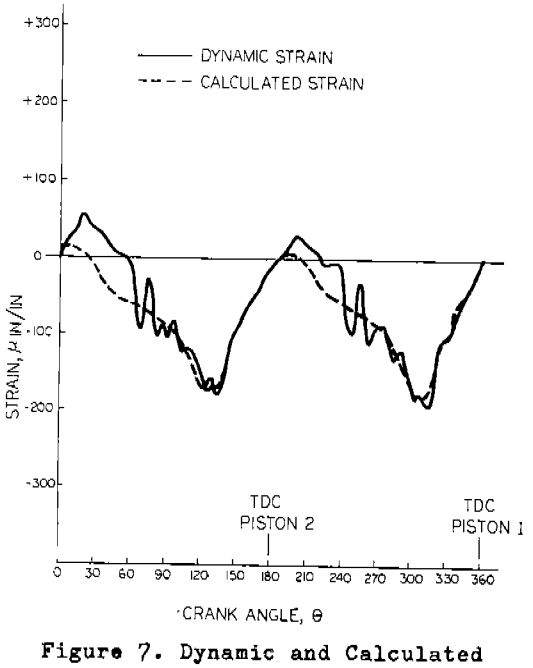

Figure 7. Dynamic and Calculated Strain at Location 2.